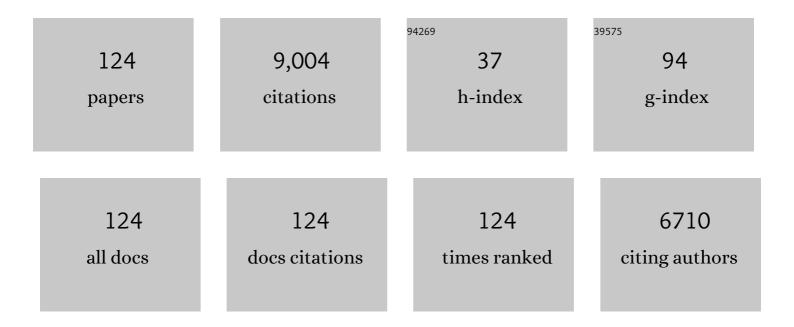
List of Publications by Year in descending order

Source: https://exaly.com/author-pdf/2309840/publications.pdf Version: 2024-02-01



| # | Article | IF | CITATIONS |
|----|---------------------------------------------------------------------------------------------------------------------------------------------------------------------------------------|------|-----------|
| 1 | Graphene Mode-Locked Ultrafast Laser. ACS Nano, 2010, 4, 803-810. | 7.3 | 1,795 |
| 2 | Nanotube–Polymer Composites for Ultrafast Photonics. Advanced Materials, 2009, 21, 3874-3899. | 11.1 | 778 |
| 3 | Wideband-tuneable, nanotube mode-locked, fibre laser. Nature Nanotechnology, 2008, 3, 738-742. | 15.6 | 596 |
| 4 | Graphene Q-switched, tunable fiber laser. Applied Physics Letters, 2011, 98, . | 1.5 | 402 |
| 5 | Sub 200 fs pulse generation from a graphene mode-locked fiber laser. Applied Physics Letters, 2010, 97, . | 1.5 | 398 |
| 6 | A stable, wideband tunable, near transform-limited, graphene-mode-locked, ultrafast laser. Nano Research, 2010, 3, 653-660. | 5.8 | 351 |
| 7 | Versatile multi-wavelength ultrafast fiber laser mode-locked by carbon nanotubes. Scientific Reports, 2013, 3, 2718. | 1.6 | 280 |
| 8 | Tm-doped fiber laser mode-locked by graphene-polymer composite. Optics Express, 2012, 20, 25077. | 1.7 | 272 |
| 9 | Planar carbon nanotube–graphene hybrid films for high-performance broadband photodetectors. Nature Communications, 2015, 6, 8589. | 5.8 | 258 |
| 10 | Two-dimensional material-based saturable absorbers: towards compact visible-wavelength all-fiber pulsed lasers. Nanoscale, 2016, 8, 1066-1072. | 2.8 | 246 |
| 11 | A self-powered high-performance graphene/silicon ultraviolet photodetector with ultra-shallow junction: breaking the limit of silicon?. Npj 2D Materials and Applications, 2017, 1, . | 3.9 | 211 |
| 12 | A light-stimulated synaptic device based on graphene hybrid phototransistor. 2D Materials, 2017, 4, 035022. | 2.0 | 186 |
| 13 | A robust and tuneable mid-infrared optical switch enabled by bulk Dirac fermions. Nature Communications, 2017, 8, 14111. | 5.8 | 174 |
| 14 | Graphene Q-switched 278Âμ m Er^3+-doped fluoride fiber laser. Optics Letters, 2013, 38, 3233. | 1.7 | 152 |
| 15 | Carbon Nanotube Polycarbonate Composites for Ultrafast Lasers. Advanced Materials, 2008, 20, 4040-4043. | 11.1 | 148 |
| 16 | Ultrafast stretched-pulse fiber laser mode-locked by carbon nanotubes. Nano Research, 2010, 3, 404-411. | 5.8 | 133 |
| 17 | Graphene Hybrid Structures for Integrated and Flexible Optoelectronics. Advanced Materials, 2020, 32, e1902039. | 11.1 | 127 |
| 18 | 74-fs nanotube-mode-locked fiber laser. Applied Physics Letters, 2012, 101, 153107. | 1.5 | 122 |

| # | Article | IF | CITATIONS |
|----|-----------------------------------------------------------------------------------------------------------------------------------------------------------------------------------------|------|-----------|
| 19 | Graphene Mode-Locked Fiber Laser at 2.8 <inline-formula> <tex-math notation="LaTeX">\$mu ext{m}\$ </tex-math></inline-formula> . IEEE Photonics Technology Letters, 2016, 28, 7-10. | 1.3 | 119 |
| 20 | A compact, high power, ultrafast laser mode-locked by carbon nanotubes. Applied Physics Letters, 2009, 95, . | 1.5 | 114 |
| 21 | L -band ultrafast fiber laser mode locked by carbon nanotubes. Applied Physics Letters, 2008, 93, . | 1.5 | 106 |
| 22 | Flexible high-repetition-rate ultrafast fiber laser. Scientific Reports, 2013, 3, 3223. | 1.6 | 106 |
| 23 | Sensitive and Ultrabroadband Phototransistor Based on Twoâ€Dimensional Bi ₂ O ₂ Se Nanosheets. Advanced Functional Materials, 2019, 29, 1905806. | 7.8 | 106 |
| 24 | An Ultrabroadband Midâ€Infrared Pulsed Optical Switch Employing Solutionâ€Processed Bismuth Oxyselenide. Advanced Materials, 2018, 30, e1801021. | 11.1 | 96 |
| 25 | Improving the Performance of Graphene Phototransistors Using a Heterostructure as the Light-Absorbing Layer. Nano Letters, 2017, 17, 6391-6396. | 4.5 | 87 |
| 26 | Carbon Nanotube Mode-Locked Thulium Fiber Laser With 200 nm Tuning Range. Scientific Reports, 2017, 7, 45109. | 1.6 | 83 |
| 27 | Double-Wall Carbon Nanotubes for Wide-Band, Ultrafast Pulse Generation. ACS Nano, 2014, 8, 4836-4847. | 7.3 | 66 |
| 28 | Graphene-carbon nanotube hybrid films for high-performance flexible photodetectors. Nano Research, 2017, 10, 1880-1887. | 5.8 | 64 |
| 29 | Three-dimensional Dirac semimetal thin-film absorber for broadband pulse generation in the near-infrared. Optics Letters, 2018, 43, 1503. | 1.7 | 52 |
| 30 | \$2-mu\$ m Wavelength Grating Coupler, Bent Waveguide, and Tunable Microring on Silicon Photonic MPW. IEEE Photonics Technology Letters, 2018, 30, 471-474. | 1.3 | 48 |
| 31 | Sensitive and Robust Ultraviolet Photodetector Array Based on Self-Assembled Graphene/C ₆₀ Hybrid Films. ACS Applied Materials & Interfaces, 2018, 10, 38326-38333. | 4.0 | 48 |
| 32 | Pulse dynamics in carbon nanotube mode-locked fiber lasers near zero cavity dispersion. Optics Express, 2015, 23, 9947. | 1.7 | 46 |
| 33 | Ultrafast saturable absorption in TiS ₂ induced by non-equilibrium electrons and the generation of a femtosecond mode-locked laser. Nanoscale, 2018, 10, 9608-9615. | 2.8 | 46 |
| 34 | Fast Photoelectric Conversion in the Nearâ€Infrared Enabled by Plasmonâ€Induced Hotâ€Electron Transfer. Advanced Materials, 2019, 31, e1903829. | 11.1 | 44 |
| 35 | Broadband hot-carrier dynamics in three-dimensional Dirac semimetal Cd3As2. Applied Physics Letters, 2017, 111, 091101. | 1.5 | 42 |
| 36 | Generation of ultra-fast laser pulses using nanotube mode-lockers. Physica Status Solidi (B): Basic Research, 2006, 243, 3551-3555. | 0.7 | 40 |

| # | Article | IF | CITATIONS |
|----|---------------------------------------------------------------------------------------------------------------------------------------------------------------------------------------------------|-----|-----------|
| 37 | Modulation of photocarrier relaxation dynamics in two-dimensional semiconductors. Light: Science and Applications, 2020, 9, 192. | 7.7 | 40 |
| 38 | Ultrafast nonlinear photoresponse of single-wall carbon nanotubes: a broadband degenerate investigation. Nanoscale, 2016, 8, 9304-9309. | 2.8 | 39 |
| 39 | Dirac semimetal saturable absorber with actively tunable modulation depth. Optics Letters, 2019, 44, 582. | 1.7 | 38 |
| 40 | Charge transfer at carbon nanotube–graphene van der Waals heterojunctions. Nanoscale, 2016, 8, 12883-12886. | 2.8 | 37 |
| 41 | Ultrafast free carrier dynamics in black phosphorus–molybdenum disulfide (BP/MoS ₂) heterostructures. Nanoscale Horizons, 2019, 4, 1099-1105. | 4.1 | 36 |
| 42 | Nanotube mode-locked, wavelength and pulsewidth tunable thulium fiber laser. Optics Express, 2019, 27, 3518. | 1.7 | 35 |
| 43 | Tuning the transport behavior of centimeter-scale WTe2 ultrathin films fabricated by pulsed laser deposition. Applied Physics Letters, 2017, 111, . | 1.5 | 34 |
| 44 | 500fs wideband tunable fiber laser mode-locked by nanotubes. Physica E: Low-Dimensional Systems and Nanostructures, 2012, 44, 1078-1081. | 1.3 | 33 |
| 45 | Broadband photocarrier dynamics and nonlinear absorption of PLD-grown WTe2 semimetal films. Applied Physics Letters, 2018, 112, . | 1.5 | 31 |
| 46 | Atomic-Scale Interfacial Magnetism in Fe/Graphene Heterojunction. Scientific Reports, 2015, 5, 11911. | 1.6 | 30 |
| 47 | Planar graphene-C60-graphene heterostructures for sensitive UV-Visible photodetection. Carbon, 2019, 146, 486-490. | 5.4 | 30 |
| 48 | Carbon nanotubes for ultrafast photonics. Physica Status Solidi (B): Basic Research, 2007, 244, 4303-4307. | 0.7 | 29 |
| 49 | Two-dimensional materials for ultrafast lasers. Chinese Physics B, 2017, 26, 034202. | 0.7 | 28 |
| 50 | Enhanced Photocatalytic Activity of 2H-MoSe ₂ by 3d Transition-Metal Doping. Journal of Physical Chemistry C, 2018, 122, 26570-26575. | 1.5 | 28 |
| 51 | Fabrication, characterization and mode locking application of single-walled carbon nanotube/polymer composite saturable absorbers. International Journal of Material Forming, 2008, 1, 107. | 0.9 | 27 |
| 52 | Tailoring exciton dynamics of monolayer transition metal dichalcogenides by interfacial electron-phonon coupling. Communications Physics, 2019, 2, . | 2.0 | 27 |
| 53 | 716  nm deep-red passively Q-switched Pr:ZBLAN all-fiber laser using a carbon-nanotube saturable absorber. Optics Letters, 2017, 42, 671. | 1.7 | 26 |
| 54 | Broadband nonlinear optical response of monolayer MoSe2 under ultrafast excitation. Applied Physics Letters, 2018, 112, . | 1.5 | 25 |

| # | Article | IF | CITATIONS |
|----|--------------------------------------------------------------------------------------------------------------------------------------------------------------------------|-----|-----------|
| 55 | Indium selenide film: a promising saturable absorber in 3- to 4-μm band for mid-infrared pulsed laser. Nanophotonics, 2020, 9, 2045-2052. | 2.9 | 25 |
| 56 | Bidirectional Red-Light Passively Q-Switched All-Fiber Ring Lasers With Carbon Nanotube Saturable Absorber. Journal of Lightwave Technology, 2018, 36, 2694-2701. | 2.7 | 23 |
| 57 | Coupled relaxation channels of excitons in monolayer MoSe ₂ . Nanoscale, 2017, 9, 18546-18551. | 2.8 | 22 |
| 58 | Soliton fiber laser modeâ€locked by a singleâ€wall carbon nanotubeâ€polymer composite. Physica Status Solidi (B): Basic Research, 2008, 245, 2319-2322. | 0.7 | 21 |
| 59 | Graphene mode-locked femtosecond Cr^2+:ZnS laser with ~300 nm tuning range. Optics Express, 2016, 24, 20774. | 1.7 | 21 |
| 60 | Third harmonic generation in Dirac semimetal Cd3As2. Applied Physics Letters, 2020, 117, . | 1.5 | 21 |
| 61 | Slowing down photocarrier relaxation in Dirac semimetal Cd ₃ As ₂ via Mn doping. Optics Letters, 2019, 44, 4103. | 1.7 | 20 |
| 62 | Recent advances in graphene and black phosphorus nonlinear plasmonics. Nanophotonics, 2020, 9, 1695-1715. | 2.9 | 19 |
| 63 | InAs-Nanowire-Based Broadband Ultrafast Optical Switch. Journal of Physical Chemistry Letters, 2019, 10, 4429-4436. | 2.1 | 18 |
| 64 | Stable Gain-Switched Thulium Fiber Laser With 140-nm Tuning Range. IEEE Photonics Technology Letters, 2016, 28, 1340-1343. | 1.3 | 17 |
| 65 | Robust, flexible and broadband photodetectors based on van der Waals graphene/C60 heterostructures. Carbon, 2020, 167, 668-674. | 5.4 | 17 |
| 66 | Layered Semiconductor Bi ₂ O ₂ Se for Broadband Pulse Generation in the Near-Infrared. IEEE Photonics Technology Letters, 2019, 31, 1056-1059. | 1.3 | 16 |
| 67 | Progress on mid-IR graphene photonics and biochemical applications. Frontiers of Optoelectronics, 2016, 9, 259-269. | 1.9 | 15 |
| 68 | Highly Sensitive and Ultrafast Organic Phototransistor Based on Rubrene Single Crystals. ACS Applied Materials & Interfaces, 2021, 13, 57735-57742. | 4.0 | 15 |
| 69 | Photoresponsivity of an all-semimetal heterostructure based on graphene and WTe2. Scientific Reports, 2018, 8, 12840. | 1.6 | 14 |
| 70 | 20 GHz actively mode-locked thulium fiber laser. Optics Express, 2018, 26, 25769. | 1.7 | 14 |
| 71 | Pushing Optical Switch into Deep Mid-Infrared Region: Band Theory, Characterization, and Performance of Topological Semimetal Antimonene. ACS Nano, 2021, 15, 7430-7438. | 7.3 | 13 |
| 72 | Spin-ARPES EUV Beamline for Ultrafast Materials Research and Development. Applied Sciences (Switzerland), 2019, 9, 370. | 1.3 | 12 |

| # | Article | IF | CITATIONS |
|----|------------------------------------------------------------------------------------------------------------------------------------------------------------------------------------------|-----|-----------|
| 73 | Enhancing photocatalytic activity in monolayer MoS2 by charge compensated co-doping with P and Cl: First principles study. Molecular Catalysis, 2019, 468, 94-99. | 1.0 | 12 |
| 74 | Two-dimensional Au & Ag hybrid plasmonic nanoparticle network: broadband nonlinear optical response and applications for pulsed laser generation. Nanophotonics, 2020, 9, 2537-2548. | 2.9 | 12 |
| 75 | Harmonic Generation in Lowâ€Dimensional Materials. Advanced Optical Materials, 2022, 10, . | 3.6 | 12 |
| 76 | All-Fiber Passively Q-Switched Laser Based on Tm3+-Doped Tellurite Fiber. IEEE Photonics Technology Letters, 2015, 27, 689-692. | 1.3 | 10 |
| 77 | Bandgap renormalization in single-wall carbon nanotubes. Scientific Reports, 2017, 7, 11221. | 1.6 | 10 |
| 78 | Hot carrier relaxation in three dimensional gapped Dirac semi-metals. Journal Physics D: Applied Physics, 2018, 51, 015101. | 1.3 | 10 |
| 79 | Observation of bimolecular recombination in high mobility semiconductor Bi2O2Se using ultrafast spectroscopy. Applied Physics Letters, 2018, 113, 061104. | 1.5 | 10 |
| 80 | Electrically and Magnetically Tunable Valley Polarization in Monolayer MoSe ₂ Proximitized by a 2D Ferromagnetic Semiconductor. Advanced Functional Materials, 2022, 32, . | 7.8 | 10 |
| 81 | Phosphorus doping effect on linear and nonlinear optical properties of Si/SiO_2 multilayers. Optical Materials Express, 2017, 7, 304. | 1.6 | 7 |
| 82 | Manipulating valley-polarized photoluminescence of MoS2 monolayer at off resonance wavelength with a double-resonance strategy. Applied Physics Letters, 2021, 119, 031106. | 1.5 | 7 |
| 83 | All-carbon hybrids for high-performance electronics, optoelectronics and energy storage. Science China Information Sciences, 2019, 62, 1. | 2.7 | 6 |
| 84 | Probing the mode-locking pattern in the parameter space of a Figure-9 laser. Optics Letters, 2022, 47, 2606. | 1.7 | 6 |
| 85 | 2- \$mu\$ m Repetition-Rate Tunable (1–6 GHz) Picosecond Source. IEEE Photonics Technology Letters, 2017, 29, 2234-2237. | 1.3 | 5 |
| 86 | Magnetism in monolayer InSe by nonmetal doping: First-principles study. Solid State Communications, 2019, 288, 56-59. | 0.9 | 5 |
| 87 | Bi ₂ O ₂ Se/Au-Based Schottky Phototransistor With Fast Response and Ultrahigh Responsivity. IEEE Electron Device Letters, 2020, 41, 1464-1467. | 2.2 | 5 |
| 88 | Controlling relaxation dynamics of excitonic states in monolayer transition metal dichalcogenides WS2 through interface engineering. Applied Physics Letters, 2021, 118, 121104. | 1.5 | 5 |
| 89 | High energy (>40 nJ), sub-100 fs, 950 nm laser for two-photon microscopy. Optics Express, 2021, 29, 38979. | 1.7 | 5 |
| 90 | Ultrafast lattice and electronic dynamics in single-walled carbon nanotubes. Nanoscale Advances, 2020, 2, 2808-2813. | 2.2 | 4 |

0

| # | Article | IF | CITATIONS |
|-----|----------------------------------------------------------------------------------------------------------------------------------------------------------------------------------------------------------------------|--------------------|-----------|
| 91 | 950 nm Femtosecond Laser by Directly Frequency-Doubling of a Thulium-Doped Fiber Laser. IEEE Photonics Technology Letters, 2022, 34, 498-501. | 1.3 | 4 |
| 92 | Coherent vibrational dynamics of <mml:math xmlns:mml="http://www.w3.org/1998/Math/MathML"><mml:msub><mml:mi>NbO</mml:mi><mml:mn>2film. Physical Review Materials, 2022, 6, .</mml:mn></mml:msub></mml:math | ıl:m o x/mı | ml:ໝsub> |
| 93 | Pulsed Lasers: An Ultrabroadband Mid-Infrared Pulsed Optical Switch Employing Solution-Processed Bismuth Oxyselenide (Adv. Mater. 31/2018). Advanced Materials, 2018, 30, 1870233. | 11.1 | 2 |
| 94 | Magnetic anisotropy of half-metallic Co2FeAl ultra-thin films epitaxially grown on GaAs(001). AIP Advances, 2019, 9, 065002. | 0.6 | 2 |
| 95 | Observation of Small Polaron and Acoustic Phonon Coupling in Ultrathin La 0.7 Sr 0.3 MnO 3 /SrTiO 3 Structures. Physica Status Solidi - Rapid Research Letters, 2019, 13, 1800657. | 1.2 | 2 |
| 96 | 10â€GHz regeneratively mode-locked thulium fiber laser with a stabilized repetition rate. Optics Express, 2021, 29, 37695. | 1.7 | 2 |
| 97 | Sub-Femtosecond Timing Jitter From a SESAM Mode-Locked Yb-Fiber Laser. IEEE Photonics Technology Letters, 2021, 33, 1309-1312. | 1.3 | 2 |
| 98 | Characteristics of saturable absorption of MoS2 films in the visible to near-infrared range. , 2014, , . | | 1 |
| 99 | Ultrafast nonlinear absorption in SWNTs: An ultra-broadband investigation. , 2015, , . | | 1 |
| 100 | Weak Anti-Localization and Quantum Oscillations in Topological Crystalline Insulator PbTe. Chinese Physics Letters, 2017, 34, 026201. | 1.3 | 1 |
| 101 | 1550 nm Compatible Ultrafast Photoconductive Material Based on a GaAs/ErAs/GaAs Heterostructure. Advanced Optical Materials, 2021, 9, 2100062. | 3.6 | 1 |
| 102 | Broadband Nonlinear Photoresponse of Monolayer MoSe2. , 2016, , . | | 1 |
| 103 | Three-dimensional Dirac semimetal Cd3As2 as high-performance 2-5 μm saturable absorbers. , 2016, , . | | 1 |
| 104 | Different ultrafast dynamics of neutral and charged excitons in monolayer WS2. , 2020, , . | | 1 |
| 105 | Light-activated artificial synapses based on graphene hybrid phototransistors. , 2016, , . | | 1 |
| 106 | Ultrafast Mid-IR carrier dynamics in three-dimensional dirac semimetal Cd <inf>3</inf> AS <inf>2</inf> . , 2015, , . | | 0 |
| 107 | Resolving the optical modulation mechanism of graphene-hybridized plasmonic metamaterials. , 2015, , . | | 0 |
| | | | _ |

Long-cavity nanosecond thulium fiber laser: A compact source of energetic mid-IR pulses. , 2015, , .

| # | Article | IF | CITATIONS |
|-----|---------------------------------------------------------------------------------------------------------------------------------------------------------|-----|-----------|
| 109 | Bandwidth Tunable, Dispersion-managed Mode-locked Thulium/holmium Fiber Laser. , 2018, , . | | Ο |
| 110 | Novel Optoelectronic Devices based on Planar Graphene-Nanotube Hybrid Film. , 2016, , . | | 0 |
| 111 | All-carbon flexible photodetectors. , 2017, , . | | О |
| 112 | High repetition-rate 2 μm ultrafast source for data communication and processing. , 2017, , . | | 0 |
| 113 | Photonic synaptic device capable of optical memory and logic operations. , 2017, , . | | О |
| 114 | Light-actuation of carbon nanotubes in liquids. , 2018, , . | | 0 |
| 115 | 15 GHz actively mode-locked fiber laser at 2 micron. , 2018, , . | | О |
| 116 | Nonlinear Reflectance of Planar Plasmonic Nanostructure. , 2018, , . | | 0 |
| 117 | Mid-infrared saturable absorber mirror (MIR-SAM) based on Dirac semimetal thin films. , 2018, , . | | Ο |
| 118 | Spectroscopic signature of interlayer coupling in Black phosphorus-graphite heterostructure. , 2018, , | | 0 |
| 119 | Third Harmonic Generation (THG) in Three-Dimensional Dirac Semimetal Cd3As2. , 2020, , . | | Ο |
| 120 | A SESAM-like Device Operating beyond 3 Micron. , 2020, , . | | 0 |
| 121 | 2 μm Actively Mode-locked External-cavity Semiconductor Laser. , 2020, , . | | Ο |
| 122 | 2 GHz Regeneratively Mode-locked Laser at 2 Micron. , 2020, , . | | 0 |
| 123 | QCL-seeded femtosecond optical parametric amplifier operating beyond 4.5 î½m. , 2021, , . | | Ο |
| 124 | Observation of an anisotropic ultrafast spin relaxation process in large-area WTe ₂ films. Journal of Applied Physics, 2022, 131, 163903. | 1.1 | 0 |